



ELSEVIER

22 October 2001

Physics Letters A 289 (2001) 207–212

PHYSICS LETTERS A

www.elsevier.com/locate/pla

Theory of Doppler-free spectroscopy with λ -thick vapor cells

A.N. Naumov ^a, A.A. Podshivalov ^a, K.N. Drabovich ^a, R.B. Miles ^b,
A.M. Zheltikov ^{a,*}

^a *International Laser Center, Faculty of Physics, Moscow State University, Moscow 119899, Russia*

^b *Department of Mechanical and Aerospace Engineering, Princeton University, Princeton, NJ 08544-5263, USA*

Received 19 July 2001; accepted 27 August 2001

Communicated by V.M. Agranovich

Abstract

A simple model of the Voigt spectral profile is employed to analyze the influence of the sizes of a vapor cell on the shape of the spectral contour of the linear susceptibility. The width of a resonant spectral line observed in transmission and absorption spectra measured with such a vapor cell is shown to tend to the natural width as one of the sizes of the vapor cell approaches the wavelength of the spectral line. The possibility of using λ -thick vapor cells, as well as one- and two-dimensional photonic band-gap structures for high resolution measurements is discussed. © 2001 Published by Elsevier Science B.V.

PACS: 32.70.Jz; 42.79.Ci; 42.25.Bs

Keywords: Thin vapor cell; Spectral line shape

1. Introduction

Doppler broadening of spectral lines is a key issue in many areas of high-resolution spectroscopy, optical frequency metrology, and optical frequency standards. There are several standard ways to alleviate problems related to Doppler broadening widely used in ultrahigh-resolution spectroscopic measurements. The use of nonlinear optical processes in counter-propagating beams [1,2], hole burning [2–4], measurements on slow, cold, and trapped particles [5–7], laser spectroscopy of forbidden transitions [3,5], and spectroscopy of Ramsey fringes [5,8] are among the most widespread methods of high-resolution spectroscopy.

A simple approach to sub-Doppler measurements with a room-temperature gas has been recently proposed by Briaudeau et al. [9,10], who observed sub-Doppler features in transmission spectra of a low-pressure vapor filling a commercially available thin glass cell with a thickness of 10–100 μm , thus extending the pillbox-cavity approach to microwave spectroscopy, proposed and experimentally implemented by Romer and Dicke back in 1955 [11], to the optical range.

In this Letter, we will examine the extension of the approach proposed by Briaudeau et al. [10] to anisotropic vapor cells with one of the sizes reduced to a characteristic scale of optical wavelength (Fig. 1(a)). Cells of this type and even one- and two-dimensional arrays of such cells (often arranged in periodic structures, called photonic band-gap structures, see Fig. 1(b)) can be fabricated by means of modern technologies. We will employ a simple model of inhomogeneous spectral broadening to analyze the influence of

* Corresponding author.

E-mail address: zheltikov@top.phys.msu.su (A.M. Zheltikov).

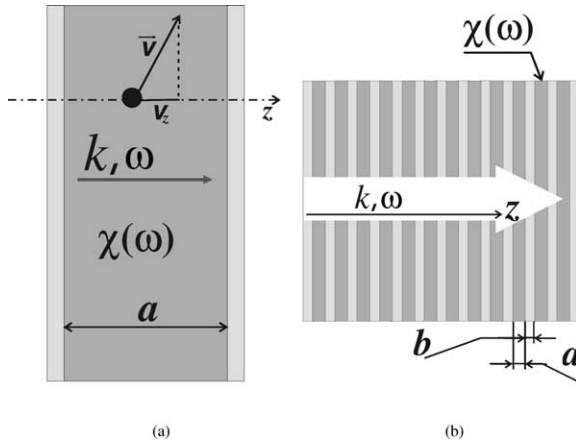


Fig. 1. An ultrathin vapor cell (a) and an array of such vapor cells arranged in a periodic one-dimensional (photonic band-gap) structure (b): a is the thickness of the cell; b is the thickness of cell walls; k and ω are the wave number and the frequency of incident light, respectively; $\chi(\omega)$ is the linear susceptibility of the resonant gas filling the cell; v is the velocity of a gas species; and v_z its projection on the z -axis, which is chosen along the direction corresponding to the minimum size of the cell.

the sizes of a vapor cell on the shape of the spectral contour of the linear susceptibility. This analysis shows that the width of a resonant spectral line observed in transmission spectra measured in the direction perpendicular to the larger dimension of the cell tends to its natural width as one of the sizes of the vapor cell approaches the wavelength of the spectral line.

2. The main idea: spectral and time-domain approaches

In this section, we shall illustrate our main idea of sub-Doppler measurements with a laser beam shining on an anisotropic vapor cell where, similar to the Romer–Dicke pillbox-cavity approach to microwave spectroscopy [11], one of the sizes is very small. The gas-cell design is shown in Fig. 1(a). The z -axis is chosen along the direction where the size of the cell reaches its minimum value a . Then, it is natural to assume that the frequency of collisions of gas species with the cell walls depends on the z -projection of the velocity of gas species and to start with an expression for a velocity-dependent Voigt spectral profile of the

linear susceptibility [12]:

$$\chi(\omega) = \frac{(n_a - n_b)\mu_{ba}\mu_{ab}}{\hbar} \times \int \frac{f(v_z)}{\omega_0 - \omega + kv_z - i\gamma(v_z)} dv_z, \quad (1)$$

where n_a and n_b are the populations of upper and lower resonant levels, μ_{ab} and μ_{ba} are the matrix elements of the electric dipole moment, ω_0 is the transition frequency, $f(v_z)$ is the distribution function of velocity projections on the z -axis, k is the wave number of incident light, and γ is the spectral width depending on the velocity v_z .

Our next key assumption is that the total spectral width γ for a group of gas species with the z -component of their velocities equal to v_z can be represented in our geometry as a sum of the natural spectral width γ_0 and a velocity-dependent part γ_1 of the spectral width, which can be written in its turn as $\gamma_1 = v_z/a$:

$$\gamma(v_z) = \gamma_0 + |v_z|/a. \quad (2)$$

Thus, we assume that gas species with higher values of $|v_z|$ collide with the cell walls more often and are, therefore, characterized by a more considerable spectral broadening than gas species with lower $|v_z|$. Since the number of particles in the cell remains constant, this implies that the contribution of such particles to the absorption of light around the line center decreases, allowing sub-Doppler features to be observed at the center of the transmission spectrum. These spectral features free of Doppler broadening are obviously related to gas species possessing minimum values of $|v_z|$, i.e., moving perpendicular to the z -axis.

Writing Eq. (2), we assume, of course, that collisions with cell walls play much more important role than collisions between gas species. This assumption imposes a limitation on the vapor pressure in the cell. In particular, the pressure of a saturated cesium vapor at room temperature is 10^{-4} Pa [13]. The mean free path length of cesium atoms under these conditions can be estimated as $3.5 \mu\text{m}$, which means that the resonance wavelength is much shorter than the mean free path under the above-specified conditions and Doppler-free measurements can be performed even at room temperature. The absorption coefficient of Cs vapor at 852 nm in such a situation can be estimated as 1.3 cm^{-1} , which implies that the use of vapor-cell arrays may be preferable in this case to achieve a no-

ticeable change in the amplitude of the signal passing through a rarefied gas. Nanochannel glass plates [14] and holey-fiber-type structures [15–17] can be employed for this purpose, as will be discussed in greater detail below in Section 3.

A physically instructive way of looking at the spectral-line narrowing problem in the above-specified geometry is to employ the time-domain approach. To understand changes arising in the spectrum of a resonant line due to the influence of the gas-cell walls in terms of the time-domain approach, we consider a group of gas species with a projection v_z on the z -axis (Fig. 1) and calculate the time evolution of the impulse response (or the time-domain linear optical susceptibility [8]) of this group of particles, i.e., the response of this ensemble to a δ -shaped optical pulse of a light wave propagating along the z -axis (Fig. 1(b)), averaged over the cell volume. We will take the attitude of Romer and Dicke [11] by assuming that collision with a cell wall transfers a particle to the state of thermal equilibrium, or at least disturbs the phase of its oscillating moment, so that particles provide no contribution to radiation after collisions with the walls. We also ignore collisions with other particles (for time-domain modeling of processes influencing the shape of spectral lines in high-density molecular gases, see, e.g., [18]) and radiation damping. Thus, the macroscopic polarization responsible for radiation is proportional to the density $n(v_z)$ of particles that have never collided the wall since the initial moment of time. Assuming that these particles are characterized by a uniform distribution in the coordinate z , we arrive at

$$n(v_z) = \begin{cases} n_0(v_z)(1 - v_z t/a), & v_z t/a < 1, \\ 0, & v_z t/a > 1, \end{cases} \quad (3)$$

where $n_0(v_z)$ is the density of particles whose velocity projection on the z -axis is equal to v_z . The impulse-response function averaged over all the particles can be then represented as

$$\hat{\chi}(t) = \int \hat{\chi}_v(t) n(t, v_z) dv, \quad (4)$$

where $\hat{\chi}_v(t)$ is the time-domain linear susceptibility of a single particle whose velocity projection on the z -axis is equal to v_z in the absence of collisions.

It is instructive to compare Eq. (4) for $\hat{\chi}(t)$ with the time-domain susceptibility $\hat{\chi}_L(t)$ obtained by taking the Fourier transform of Eq. (1) for the Voigt contour

of $\chi(\omega)$, which corresponds to the Lorentz model of the frequency-domain susceptibility of a single particle. Applying the Fourier transform to Eq. (1), we derive

$$\hat{\chi}_L(t) = \int \hat{\chi}_{vL}(t) n_L(t, v_z) dv_z, \quad (5)$$

where

$$\hat{\chi}_{vL}(t) = i \frac{\mu_{ba} \mu_{ab}}{\hbar} \exp[-i(\omega_0 + kv)t - \gamma_0 t]$$

is the Lorentz model of the time-domain susceptibility of a single particle whose velocity projection on the z -axis is equal to v_z in the absence of collisions and

$$n_L(t, v_z) = (n_a - n_b) \exp[-|v_z|t/a] f(v_z) \quad (6)$$

is the density of particles whose velocity projection on the z -axis is equal to v_z . The decrease in $n_L(t, v_z)$ as a function of time reflects the fact that the density of particles that never hit the cell walls lowers with time.

Comparing Eqs. (3) and (6), we find that the Lorentz model of the frequency-domain linear susceptibility of a single particle brings us to an exponential time dependence of the density of particles $n_L(t, v_z)$ contributing to the impulse response (the dotted curve in Fig. 3), while the time-domain approach based on Eq. (3) gives a linear time dependence of the relevant density of particles $n(t, v_z)$ (the solid curve in Fig. 3). Fig. 3, displaying the time dependences of $n(t, v_z)$ and $n_L(t, v_z)$, gives a clear idea of the differences between the time-domain approach based on Eqs. (3) and (4) and the frequency-domain approach based on the analysis of Eq. (1). However, although the predictions of these two approaches may quantitatively differ from each other, the qualitative features predicted by these models should be the same, and the time-domain (more physical in some respect) approach generally verifies the spectral approach based on Eq. (1). In particular, we will show below in Section 3 that both models give the same criterion for the appearance of sub-Doppler features in inhomogeneously broadened spectra of gases in a thin cell.

3. Results and discussion

We performed calculations of line spectral profiles assuming that the distribution of gas species in their velocity projections on the z -axis is described by a

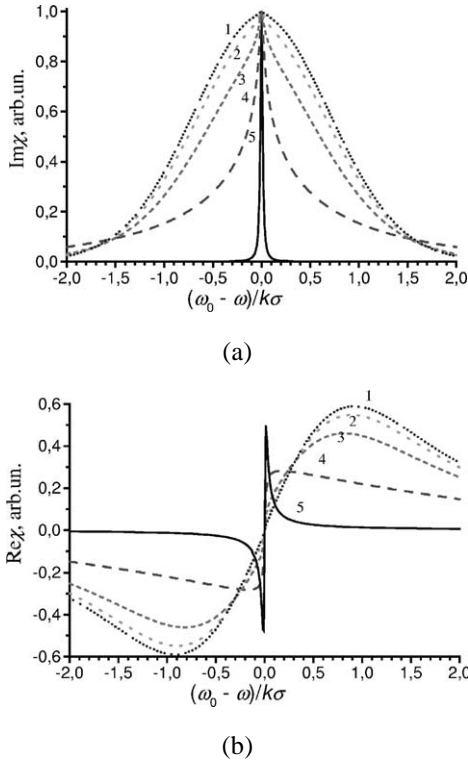


Fig. 2. The spectral profiles of the imaginary (a) and real (b) parts of the linear susceptibility calculated with the use of Eqs. (1)–(3) for the $6S_{1/2}$ – $6P_{3/2}^0$ transition of Cs atoms with a wavelength of 852 nm for $a = 10$ (1), 3 (2), 1 (3), and $0.1 \mu\text{m}$ (4) with $k\sigma/\gamma_0 = 80$ and $\gamma_0 = 1.8$ MHz, which corresponds to the temperature $T = 300$ K. The solid lines 5 display the Doppler-free spectral profiles of the imaginary and real parts of the linear susceptibility with natural widths of the considered spectral line.

Maxwellian function:

$$f(v_z) = f_0(v_z) = \frac{1}{\sigma\sqrt{\pi}} \exp\left[-\left(\frac{v_z}{\sigma}\right)^2\right], \quad (7)$$

where $\sigma = \sqrt{2k_B T/m}$, k_B is the Boltzmann constant, T is the temperature, and m is the mass of gas species.

Fig. 2 displays the spectral profiles of the imaginary (Fig. 2(a)) and real (Fig. 2(b)) parts of the linear susceptibility calculated with the use of Eqs. (1)–(3) for the $6S_{1/2}$ – $6P_{3/2}^0$ transition of Cs atoms with a wavelength of 852 nm for $a = 10$ (1), 3 (2), 1 (3), and $0.1 \mu\text{m}$ (4) with $k\sigma/\gamma_0 = 80$ and $\gamma_0 = 1.8$ MHz, which corresponds to the temperature $T = 300$ K (the hyperfine splitting was ignored in these calculations). The solid lines 5 in Figs. 2(a) and (b) display the Doppler-

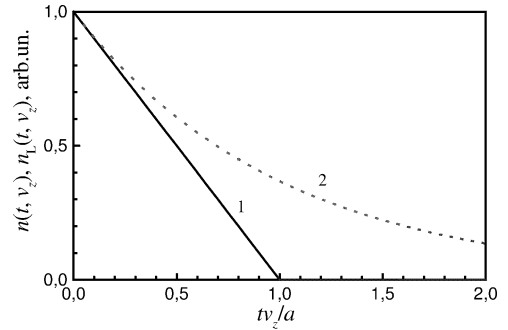


Fig. 3. Time dependences of the densities of particles $n(t, v_z)$ and $n_L(t, v_z)$ whose velocity projections on the z -axis are equal to v_z and that contribute to the impulse response of the system $\hat{\chi}(t)$ calculated with Eqs. (3) (solid line) and (6) (dotted line), respectively.

free spectral profiles of the imaginary and real parts of the linear susceptibility with natural widths of the considered spectral line. As can be seen from the results presented in these plots, the sub-Doppler structure of the spectrum around the resonance frequency becomes especially well pronounced when the size a of the cell becomes comparable with the resonance wavelength, i.e., when $ka \sim 1$ (curves 2–4). In the case when $ka \gg 1$, the spectral profile of the linear susceptibility only slightly differs from the relevant Doppler profile (curves 1 in Figs. 2(a) and (b), which correspond to $ka = 7.4$).

The fact that the spectral profile of the linear susceptibility becomes essentially sub-Doppler when the thickness of the cell becomes comparable with the resonance wavelength can be qualitatively understood in a very simple way. Doppler-free features with a natural line width become noticeable against the background of a Doppler-broadened resonance line when the line width of the spectral profile corresponding to gas species whose Doppler shift is equal to the natural width ($kv_z = \gamma_0$) considerably (say, by a factor of two, see Fig. 4) exceeds the line width of the spectral profile corresponding to species with $v_z = 0$: $\gamma_0 + v_z/a \geq 2\gamma_0$. With such a criterion, we arrive at

$$ka \leq 1. \quad (8)$$

In terms of the time-domain approach, this criterion can be understood if we estimate the phase shift incurred by a particle moving with a z -projection of the velocity v_z as $kv_z t$. Then, to reduce the contribution of particles with a large phase shift to the inhomoge-

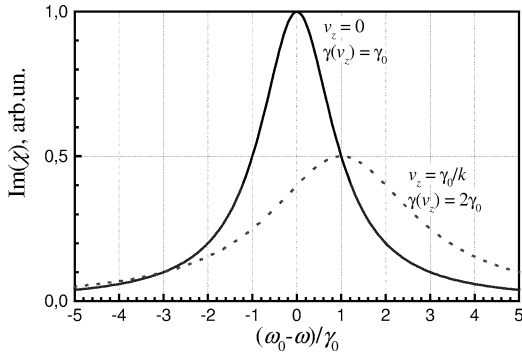


Fig. 4. Doppler-free features with a natural line width become noticeable against the background of a Doppler-broadened resonance line when the line width of the spectral profile corresponding to gas species whose Doppler shift is equal to the natural width ($kv_z = \gamma_0$, the dotted line) exceeds the line width of the spectral profile corresponding to species with $v_z = 0$ (the solid line) by a factor of two.

neously broadened spectral line, we require that all the particles with a z -projection of the velocity equal to

$$kv_z t \sim 1 \quad (9)$$

should undergo collisions with the walls, i.e.,

$$v_z t / a > 1. \quad (10)$$

Combining Eqs. (9) and (10), we arrive at the criterion of Eq. (8), which is now understood as the condition of reducing the influence of Doppler dephasing. In other words, if the inequality of Eq. (8) is satisfied and a light wave propagates along the z -axis (Fig. 1(b)), a moving particle sees a light wave whose phase remains approximately the same within the entire cell, with no additional phase shift arising for such a particle.

An important conclusion that follows from our examination is that sub-Doppler features become especially noticeable when an anisotropic vapor cell is designed in such a way that one of its sizes is on the order of the resonance wavelength. This kind of relation between the optical wavelength and the characteristic size of the structure is typical of photonic band-gap (PBG) structures [19–21]. A concept of a PBG cell seems to offer much promise for sub-Doppler spectroscopic applications also because one can benefit in this case from using many anisotropic cavities instead of only one (Fig. 1(b)), which is especially useful under conditions when the gas pressure has to be kept low in order to reduce the influence of collisional broadening

(see the estimates above). This concept can be also extended to two dimensions, bringing us to an idea of using nanochannel glass plates [14] and holey-fiber-type structures [15–17] for high-resolution spectroscopy and optical metrology applications. Although we do not need the periodicity, which is inherent in PBG structures, to perform sub-Doppler measurements, this periodicity, as shown in [22], can be employed to filter and disperse laser radiation, while a carefully designed photonic-crystal lattice of a PBG structure allows the laser guiding of atoms [23], thus offering several useful options in high-resolution experiments.

4. Conclusion

Thus, a simple model of the Voigt spectral profile employed in this Letter allowed us to analyze the influence of the sizes of a vapor cell on the shape of the spectral contour of the linear susceptibility. Gas species with higher absolute values of the transverse velocity collide with the walls of an ultrathin cell more often than gas species with lower absolute values of the transverse velocity. Since the number of particles in the cell remains constant, this implies that the contribution of such particles to the absorption of light around the line center decreases, allowing sub-Doppler features to be observed at the center of the transmission spectrum. We have shown that the width of a resonant spectral line observed in transmission and absorption spectra measured with such a vapor cell tends to the natural width as one of the sizes of the vapor cell approaches the wavelength of the spectral line. Ultrathin vapor cells designed in such a way that one of their sizes is on the order of optical wavelength may allow the observation of this effect in one dimension, while nanochannel glass plates, holey-fiber-type structures, and other two-dimensional photonic band-gap structures open the way to observe Doppler-free spectral features in two dimensions, which can be employed in high-resolution spectroscopy, optical frequency metrology, and optical frequency standards.

Acknowledgements

This work was supported in part by the President of Russian Federation Grant no. 00-15-99304 and the

Russian Foundation for Basic Research Project no. 00-02-17567. The research described in this publication was made possible in part by Award no. RP2-2266 of the US Civilian Research and Development Foundation for the Independent States of the Former Soviet Union (CRDF).

References

- [1] L.S. Vasilenko, V.P. Chebotayev, A.V. Shishaev, *JETP Lett.* 12 (1970) 113.
- [2] V.P. Chebotayev, V.S. Letokhov, *Nonlinear Laser Spectroscopy*, Springer, Berlin, 1977.
- [3] H. Walther (Ed.), *Laser Spectroscopy of Atoms and Molecules*, Springer, Berlin, 1976.
- [4] W.R. Bennett Jr., *Phys. Rev.* 126 (1962) 580; W.E. Lamb, *Phys. Rev. A* 134 (1964) 1429.
- [5] W. Demtröder, *Laser Spectroscopy*, Springer, Berlin, 1981.
- [6] V.G. Minogin, V.S. Letokhov, *Laser Light Pressure on Atoms*, Gordon and Breach, New York, 1987.
- [7] A. Ashkin, *Science* 210 (1980) 1081.
- [8] Y.R. Shen, *The Principles of Nonlinear Optics*, Wiley, New York, 1984.
- [9] S. Briaudeau, D. Bloch, M. Ducloy, *Europhys. Lett.* 35 (1996) 337.
- [10] S. Briaudeau, S. Saltiel, G. Nienhuis, D. Bloch, M. Ducloy, *Phys. Rev. A* 57 (1998) R3169.
- [11] R.H. Romer, R.H. Dicke, *Phys. Rev.* 99 (1955) 532.
- [12] A.D. May, *Phys. Rev. A* 59 (1999) 3495.
- [13] I.S. Grigor'ev, E.Z. Meilikhov (Eds.), *Handbook of Physical Quantities*, Energoatomizdat, Moscow, 1991, in Russian.
- [14] H.-B. Lin, R.J. Tonucci, A.J. Campillo, *Opt. Lett.* 23 (1998) 94.
- [15] J.C. Knight, T.A. Birks, P.St.J. Russell, D.M. Atkin, *Opt. Lett.* 21 (1996) 1547.
- [16] T.A. Birks, J.C. Knight, P.St.J. Russell, *Opt. Lett.* 22 (1997) 961; J.C. Knight, J. Broeng, T.A. Birks, P.St.J. Russell, *Science* 282 (1998) 1476.
- [17] A.M. Zheltikov, *Phys. Usp.* 170 (2000) 1125.
- [18] C.J. Meinrenken, W.D. Gillespie, S. Macheret, W.R. Lempert, R.B. Miles, *J. Chem. Phys.* 106 (1997) 8299.
- [19] E. Yablonovitch, *J. Opt. Soc. Am. B* 10 (1993) 283.
- [20] J. Joannopoulos, R. Meade, J. Winn, *Photonic Crystals*, Princeton University, Princeton, 1995.
- [21] C.M. Soukoulis (Ed.), *Photonic Band Gaps and Localization*, Plenum, New York, 1993.
- [22] A.M. Zheltikov, A.N. Naumov, P. Barker, R.B. Miles, *Opt. Spectrosc.* 89 (2000) 282.
- [23] A.V. Tarasishin, S.A. Magnitskii, V.A. Shuvaev, A.M. Zheltikov, *Opt. Commun.* 184 (2000) 391.